Modelling the performance of two-channeled haemodialyser with single rectangular membrane – Asymptotics and numerical approximation

Ugochukwu Obinna Ugwu*

Abstract— The efficiency of a two channeled haemodialyser with a rectangular membrane have been investigated; with blood flow considered incompressible, unidirectionally constant and assumed to be flowing in counter-clockwise direction with the dialysate. The smallest dimensionless parameter ε was identified and technique of asymptotic expansions used to consider a problem for the resulting 2D-convection-diffusion system (CDs) in the limit of $\varepsilon \to 0$. The CDs was solved numerically using MATLAB's *pdepe* while eigenvalues found in transcendental equation were obtained using MATLAB's *fsolve*. Comparison between the numerical and analytic solutions were considered with sensitivity analysis of diffusion coefficient α_b and membrane coefficient β_b studied.

Keywords: asymptotics, blood, concentration, convection, dialysate, diffusion, efficiency, haemodialyser, MATLAB's - *fsolve* and *pdepe* solvers, membrane.

1. Introduction

Dialysis is an artificial process of removing excess waste from the body due to kidney dysfunction. This dysfunction results in an imbalance of body's water and minerals leading to accumulation of waste which could have been excreted through the kidney. The frequenting of dialysis could be a temporal or permanent measure depending on the severity of the kidney disease.

Though there are two main types of dialysis; haemodialysis and peritoneal dialysis [1]. However, in this study, we have focused on haemodialysis which involves the removal of excess waste such as urea and creatinine by physical (external) processes of blood circulation though a haemodialyser. For the purpose of this discuss, the haemodialyser could be envisaged as a two-channeled device with single rectangular membrane.

Here, blood is pumped extracorporeally through a channel of the haemodialyser partitioned into two-halves by a semi-permeable membrane. This membrane has a known pore size distribution allowing molecules (such as urea and creatinine) below a certain size to pass through to the other half of the channel containing the dialysate by diffusion.

The dialysate (probably an ionic salt solution) is used to provide the required large enough concentration difference to ensure mass transfer driven by differences in concentration on either side of the membrane. They are discarded alongside the removed toxic waste after leaving the haemodialyser.

It is pertinent to note that blood and dialysate has been considered to be flowing in opposite sides of the channel in a counter-clockwise direction. This incredible choice was base on the fact that counter current design maximizes haemodialyser performance than concurrent design [2].

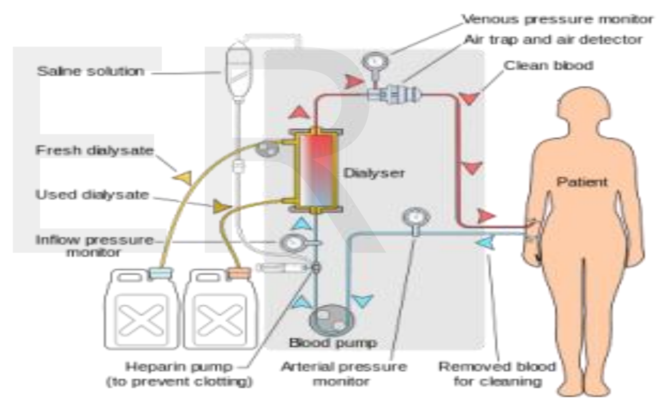

Fig. 1: Cross-section of a haemodialysis set up in a counter-clockwise direction obtained from [1].

Though haemodialysis depends heavily on the processes of diffusion and convection, the amount of waste molecules removed depends on the magnitude of the concentration gradient, the distance traveled by the molecules along the channel and the area through which diffusion takes place [2]. It suffices to say that the performance of the haemodialyser depends heavily on these factors.

Our objective is to develop a mathematical model capable of determining the efficiency of the haemodialyser i.e. to understand how best to maximize haemodialyser for optimal performance. It suffices to say that, we want to use a detailed asymptotic and numerical analysis to determine the efficiency of our device.

2. Model Formulation

Earlier we mentioned that for the purpose of this study, we have restricted to a case of two channeled device analogous to

*Graduate assistant, Department of Mathematics, University of Nigeria Nsukka. Currently undertaking MSc Modern Applications of Mathematics, Department of Mathematical Sciences, University of Bath, Bath, BA2 7AY, UK. E-mail: ugobinnah@gmail.com, uou20@bath.ac.uk

ISSN 2229-5518

the dialyser in Figure 1 with a single rectangular membrane between the channels. The device considered to be operating in a counter-clockwise direction with blood and dialysate on the opposite sides of the membrane.

2.1 Model Assumptions

1.0 The flow field is unidirectionally constant along the x-axis.
2.0 There is large enough concentration difference on both sides of the channel to allow for mass flux from blood to dialysate region only.
3.0 The semi-permeable membrane made thin enough to allow for diffusion of molecules (such urea and creatinine) of a particular size pores. This is consistent with Fick's law on diffusion.
4.0 No significant diffusion taking place along the z-direction.
5.0 The dialysate is far away from the membrane. This follows from the fact that the closer the concentration between the two regions, the longer the transit time [3].
6.0 Blood considered as an incompressible fluid.

Now, consider two distinct regions Ω_b and Ω_d called the blood and dialysate domain respectively as can be envisaged from Fig. 1. Let

$$\Omega_b = \{(x, y, z) \in \mathrm{R} : 0 < x < l, 0 < y < H, 0 < z < W\} \tag{2.1}$$

$$\Omega_d = \{(x, y, z) \in \mathrm{R} : 0 < x < l, -H < y < 0, 0 < z < W\} \tag{2.2}$$

where l, H and W are length, height and width of the channel respectively.

To address our objective, we introduce a basic reaction-diffusion model to describe the convection along the channel and diffusion across the membrane. In other words, the working of a haemodialyser is governed by convection on both sides of the channel and diffusion involving mass transfer from region of higher concentration (2.1) to the region of lower concentration (2.2).

Let $C = C(x, y, t)$: concentration of waste in blood and $F = F(x, y, t)$: concentration of waste in the dialysate. It is noteworthy that the above assumptions, in particular (4.0) simplifies the dependence of C and F on the parameters x, y, z and t to x, y and t only.

Hence, the governing convection-diffusion equation that hold within each region (2.1) and (2.2) is given by

Ω_b :

$$\frac{\partial C}{\partial t} + V_b \frac{\partial C}{\partial x} = D_b \left(\frac{\partial^2 C}{\partial x^2} + \frac{\partial^2 C}{\partial y^2}\right), \ 0 < x < 1, \ 0 < y < 1 \tag{2.3}$$

Initial Conditions (ICs):

$$t = 0 : C = 0; \quad x = 0 : C = C_i \ \left(\frac{\partial C}{\partial x} = 0\right) \tag{2.4}$$

Boundary Conditions (BCs):

$$y = 0 : D_b \frac{\partial C}{\partial y} = h(C - F) \tag{2.5a}$$

$$y = H : \ \frac{\partial C}{\partial y} = 0 \tag{2.5b}$$

Ω_d :

$$\frac{\partial F}{\partial t} + V_d \frac{\partial F}{\partial x} = D_d \left(\frac{\partial^2 F}{\partial x^2} + \frac{\partial^2 F}{\partial y^2}\right), \ 0 < x < 1, \ -1 < y < 0 \tag{2.6}$$

ICs:

$$t = 0 : F = 0; \quad x = 0 : \ F = 0 \left(\frac{\partial F}{\partial x} = 0\right) \tag{2.7}$$

BCs:

$$y = 0 : \ D_d \frac{\partial F}{\partial y} = h(C - F); \tag{2.8a}$$

$$y = -H : \ \frac{\partial F}{\partial y} = 0 \tag{2.8b}$$

TABLE 1: Typical values of the dimensional variables.

Variables	Typical values
C_i	$0.002 gm/ml$
D_b	$0.0005 cm^2/sec$
W	$20 cm$
H	$0.1 cm$
l	$80 cm$
Q_b	$2.5 cm^3/sec$
Q_d	$10 cm^3/sec$
h	$0.02 \to 0.05 cm/sec$
V_b	$1.25 cm/sec$
V_d	$5 cm/sec$

Source: The Third Mathematics-in-Medicine Study Group held at the University of Nottingham 1-13 Sept. 2002.

where C_i is the inlet concentration of blood, h is the mass transfer coefficient, $h(C - F)$ is the mass transfer rate per unit membrane area from blood to water (dialysate), V_b is the speed of blood and D_b is the diffusivity coefficient in blood. V_d is the speed of the dialysate and D_d is the diffusivity coefficient in dialysate. Q_b is the blood flow rate and Q_d is the dialysate flow rate.

It is pertinent to note that (2.5a) and (2.8a) follows from the fact the concentration profile of the membrane boundary has an associated discontinuities. The consequence is to ensure continuous flux from (2.1) into (2.2). Also to be noted is the uniformity in height of both channels.

3. Mathematical Analysis

3.1 Nondimensionalisation

To solve (2.3)-(2.8), we nondimensionalise by introducing the following scaling, where a bar is used to denote a nondimensional variable.

$$x = l\bar{x},\ \ y = H\bar{y},\ \ t = \frac{l\bar{t}}{V_b},\ \ C = C_i\bar{C},\ \ F = C_i\bar{F},\ \ t = \frac{l\bar{t}}{V_d} \tag{3.1}$$

Differentiating (3.1) and substituting accordingly into (2.3)-(2.8), we obtain

Ω_b :

$$\frac{\partial \bar{C}}{\partial \bar{t}} + \frac{\partial \bar{C}}{\partial \bar{x}} = \alpha_b\left(\varepsilon\frac{\partial^2 \bar{C}}{\partial \bar{x}^2} + \frac{\partial^2 \bar{C}}{\partial \bar{y}^2}\right) \tag{3.2}$$

ICs:

$$\bar{t} = 0: \bar{C} = 0; \quad \bar{x} = 0: \bar{C} = 1\ \left(\frac{\partial \bar{C}}{\partial \bar{x}} = 0\right) \tag{3.3}$$

BCs:

$$\bar{y} = 0: \frac{\partial \bar{C}}{\partial \bar{y}} = \beta_b(\bar{C} - \bar{F}); \quad \bar{y} = 1: \frac{\partial \bar{C}}{\partial \bar{y}} = 0 \tag{3.4}$$

Ω_d :

$$\frac{\partial \bar{F}}{\partial \bar{t}} + \frac{\partial \bar{F}}{\partial \bar{x}} = \alpha_d\left(\varepsilon\frac{\partial^2 \bar{F}}{\partial \bar{x}^2} + \frac{\partial^2 \bar{F}}{\partial \bar{y}^2}\right) \tag{3.5}$$

ICs:

$$\bar{t} = 0: \bar{F} = 0; \quad \bar{x} = 0: \bar{F} = 0\ \left(\frac{\partial \bar{F}}{\partial \bar{x}} = 0\right) \tag{3.6}$$

BCs:

$$\bar{y} = -1: \frac{\partial \bar{F}}{\partial \bar{y}} = 0; \quad \bar{y} = 0: \frac{\partial \bar{F}}{\partial \bar{y}} = \beta_b(\bar{C} - \bar{F}) \tag{3.7}$$

where

$$\alpha_b = \frac{D_b l}{H^2 V_b};\ \ \beta_b = \frac{hH}{D_b};\ \ \varepsilon = \frac{H^2}{l^2};\ \ \alpha_d = \frac{D_d l}{H^2 V_d};\ \ \beta_d = \frac{hH}{D_d} \tag{3.8}$$

Equations (3.2)-(3.7) give the dimensionless form of convection-diffusion equation in the domain Ω_b and Ω_d. $\alpha_b, \beta_b, \varepsilon, \alpha_d$ and ε are the dimensionless parameters.

From here on, we drop the bars from our variables and assume that every variable is dimensionless; focus more on the domain Ω_b with little inclination to the membrane since coupled with assumption (5.0), it has more physical realistic contribution to the performance of haemodialyser. This we hope to see in a sequel.

TABLE 2: Estimated nondimensional variables using values of Table 1.

Dimensionless variables	Typical values
α_b, α_d	3.2
β_b, β_d	$4 \rightarrow 10$
ε	1.5625×10^{-6}

3.2 Asymptotic Analysis

In this section we investigate extensively the behaviour of (3.2)-(3.4) since as shown in Table 2, $\varepsilon << 1$ $(\varepsilon \sim 10^{-6})$. Now, observe that since the system must be well-posed, we require that as $\varepsilon \rightarrow 0$, $\beta_b = O(1)$ and $\alpha_b = O(1)$ so that (3.2) becomes:

$$\frac{\partial C}{\partial t} + \frac{\partial C}{\partial x} = \alpha_b\frac{\partial^2 C}{\partial y^2} \tag{3.9}$$

ICs:

$$t = 0: C = 0; \quad x = 0: C = 1 \tag{3.10}$$

BCs:

$$y = 0: \frac{\partial C}{\partial y} = \beta_b(C - F); \quad y = 1: \frac{\partial C}{\partial y} = 0 \tag{3.11}$$

It is pertinent to note that $\frac{\partial C}{\partial x} = 0$ (no diffusive flux condition in x-direction) in (3.3) has been neglected in (3.10) since $\varepsilon\frac{\partial^2 C}{\partial x^2}$ varnished as $\varepsilon \rightarrow 0$.

Pose:

$$C = C_0 + \varepsilon C_1 + \varepsilon^2 C_2 + \ldots; F = F_0 + \varepsilon F_1 + \varepsilon^2 F_2 + \ldots \tag{3.12}$$

Differentiating (3.12) and substituting accordingly into (3.9)-(3.11) we obtain the leading order coefficients ε^0:

$$\frac{\partial C_0}{\partial t} + \frac{\partial C_0}{\partial x} = \alpha_b\frac{\partial^2 C_0}{\partial y^2} \tag{3.13}$$

ICs:

$$t = 0: C_0 = 0; \quad x = 0: C_0 = 1 \tag{3.14}$$

BCs:

$$y = 0: \frac{\partial C_0}{\partial y} = \beta_b(C_0 - F_0); \quad y = 1: \frac{\partial C_0}{\partial y} = 0 \tag{3.15}$$

Notice that (3.13)-(3.15) are coupled and since $F_0 << C_0$ by assumption (5.0), (3.15) becomes

BCs:

$$y = 0: \frac{\partial C_0}{\partial y} = \beta_b C_0; \quad y = 1: \frac{\partial C_0}{\partial y} = 0. \tag{3.16}$$

ISSN 2229-5518

Thus giving rise to the decoupled system (3.13), (3.14) and (3.16). It can be justified asymptotically that $F \equiv 0$ (F is identically zero) on the membrane.

3.3 Steady Solution

In this section, we seek an analytic solution to the decoupled system above assuming the flow is steady. i.e.

$$\frac{\partial C_0}{\partial x} = \alpha_b \frac{\partial^2 C_0}{\partial y^2} \qquad (3.17)$$

IC:

$$x = 0: \quad C_0 = 1 \qquad (3.18)$$

BCs:

$$y = 0: \quad \frac{\partial C_0}{\partial y} = \beta_b C_0; \quad y = 1: \quad \frac{\partial C_0}{\partial y} = 0 \qquad (3.19)$$

The system (3.17)-(3.19) have been solved by method of separation of variables shown in Appendix A to obtaining the fundamental solution

$$C_0(x, y) = \sum_{n=0}^{\infty} A_n \left(\frac{cos(\lambda_n (1-y))}{cos\lambda_n} \right) e^{-\alpha_b \lambda_n^2 x}$$

(3.20)

where $A_n = \dfrac{2sin(2\lambda_n)}{2\lambda_n + sin(2\lambda_n)}$.

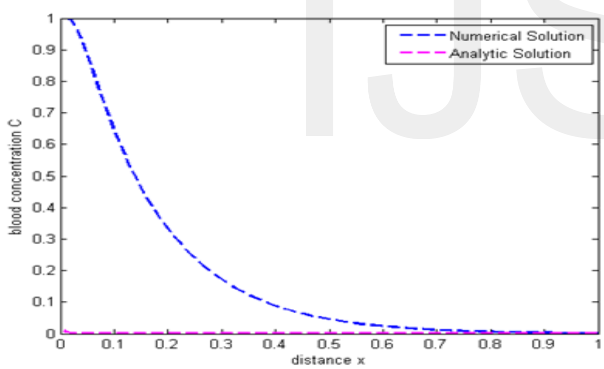

Fig. 2: Plots of analytic solution and the end column of the numerical solution matrix.

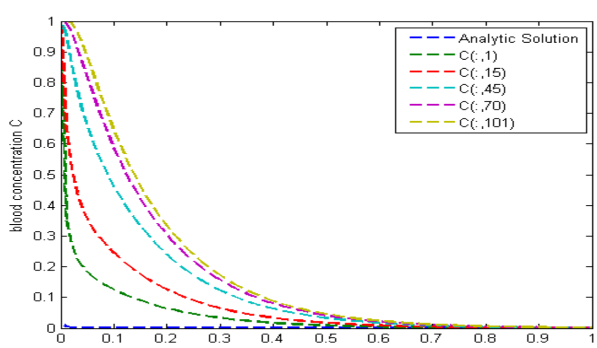

Fig. 3: Shows selected columns of the numerical solution matrix with the analytic solution. Notice that the numerical and analytic solutions do not coincide. Thus, leading to expected solution error.

TABLE 3: Set of eigenvalues obtained numerically using MATLAB's *fsolve* with $\beta_b = 8$.

s/n	λ_n
1	1.3978
2	4.2264
3	7.1263
4	10.0949
5	13.1141
6	16.1675
7	19.2435
8	22.3351
9	25.4374
10	28.5476

The eigenvalues λ_n were obtained numerically using MATLAB's *fsolve* with tolerance, $tol = 10^{-6}$. It is immediate from Table 3 that $tan\lambda_n = n\pi + correction(\varepsilon)$ and can be justified asymptotically that $\tan \lambda_n \sim n\pi$ as $n \to \infty$ (see Appendix A).

3.4 Unsteady State Solution

Again, consider the decoupled system (3.13), (3.14) and (3.16). To illustrate the transient behaviour, we define the Laplace transform of $C_0(x, y, t)$ as

$$\overline{c}(x, y; s) = \int_0^{\infty} e^{-st} C_0(x, y, t) dt \qquad (3.21)$$

Taking Laplace transform of the decoupled system and applying (3.21) gives

$$\frac{\partial v}{\partial x} = \alpha_b \frac{\partial^2 v}{\partial y^2} \qquad (3.22)$$

IC:

$$x = 0: \quad v = \frac{1}{s} \qquad (3.23)$$

BCs:

$$y = 0: \quad \frac{\partial v}{\partial y} = \beta_b v; \quad y = 1: \quad \frac{\partial v}{\partial y} = 0 \qquad (3.24)$$

where

$$v(x, y) = e^{sx} \overline{c}(x, y; s) \qquad (3.25)$$

Solve (3.22)-(3.24) by method of separation of variables and substitute into (3.25) to obtain

$$\overline{c}(x, y; s) = \sum_{n=0}^{\infty} A_n(s) \left(\frac{cos(\lambda_n (1-y))}{cos\lambda_n} \right) e^{-\alpha_b \lambda_n^2 x} e^{-sx} \qquad (3.26)$$

Imposing (3.23) on (3.26) gives

International Journal of Scientific & Engineering Research Volume 6, Issue 6, June-2015
ISSN 2229-5518

$$\bar{c}(x,y;s)=\sum_{n=0}^{\infty}A_n(s)\left(\frac{\cos\left(\lambda_n(1-y)\right)}{\cos\lambda_n}\right)=\frac{1}{s} \qquad (3.27)$$

where $A_n(s)=\frac{1}{s}\hat{A}_n$.

Next we take Laplace inverse of (3.26)-(3.27) to obtain that

$$C_0(x,y,t)=u(t-x)\sum_{n=0}^{\infty}\hat{A}_n\left(\frac{\cos\left(\lambda_n(1-y)\right)}{\cos\lambda_n}\right)e^{-\alpha_b\lambda_n^2 x} \qquad (3.28)$$

$$\sum_{n=0}^{\infty}\hat{A}_n\left(\frac{\cos\left(\lambda_n(1-y)\right)}{\cos\lambda_n}\right)=1 \qquad (3.29)$$

u is a step function defined as

$$u(t-x)=\begin{cases}1 & t\geq x\\ 0 & t<x\end{cases}$$

and $0<x<1$ as before. Notice that it will only take 1 time unit to attain steady state.

4. Discussion of Results

Here we present a detailed discussion of our results as an insight towards drawing a sensible conclusion regarding the efficiency of our device - haemodialyser.

It is evident our model equation truly describes the behaviour of blood concentration as it flows down the channel. This is immediate from Fig. 4 and 5 where the concentration of blood moves in layers having its maximum close to the base of the membrane. In fact, this suggests that different molecules travel at different convection and diffusion rates. However, this maximum concentration decreases as it gets to the end of the channel with large chunk of waste already diffused out of the channel. Interestingly, this maximum concentration at the base of the membrane could be attributed to waste molecules (such as creatinine and urea) being pulled closer and closer by the dialysate concentration on the other side of the channel.

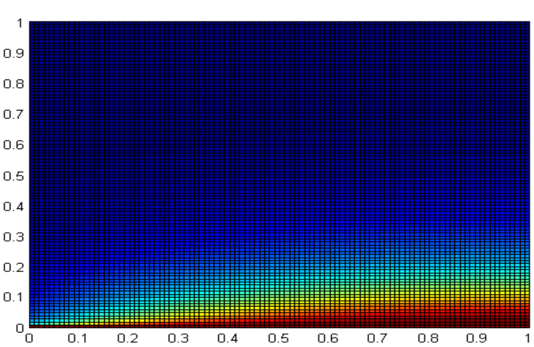

Fig. 4: superimposition of surface *surf(y, x, C)* on the plane (x, C).

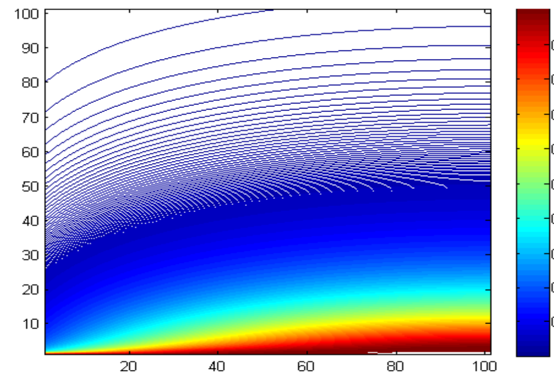

Fig. 5: Shows a contour plot of the numerical solution with height 1000 with difference layers of blood concentration as it flows down the concentration gradient diffusing through the membrane.

Of course, this is expected since by assumption 2.0, we provided a large enough concentration difference to allow for mass transfer only from Ω_b to Ω_d. With high optimism from Fig. 2 and 3, we would anticipate that at some point in the flow regime, the waste concentration out of the channel would probably be zero and that initially; it took quite some time for the membrane to completely absorb the waste before attaining steady state.

In light of the above, we see from the unsteady state solution (3.28) that within this interval of time, there are discontinuities on the membrane as blood get past the channel. Pertinently, (3.28) informs that it only took a unit time to attain steady state i.e. concentration reaches steady state in 1 time unit.

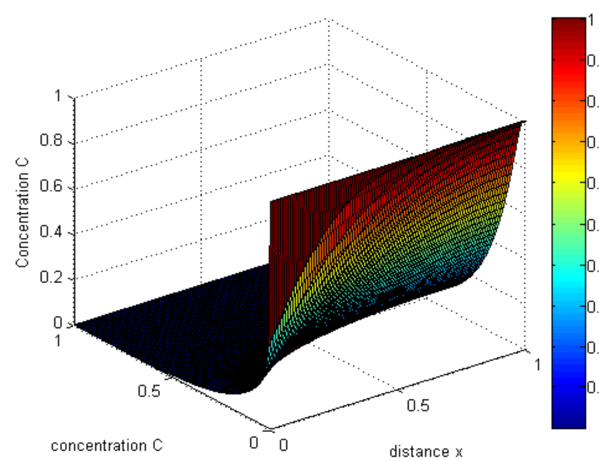

Fig. 6: 3D Surface plot of the numerical solution to steady state problem.

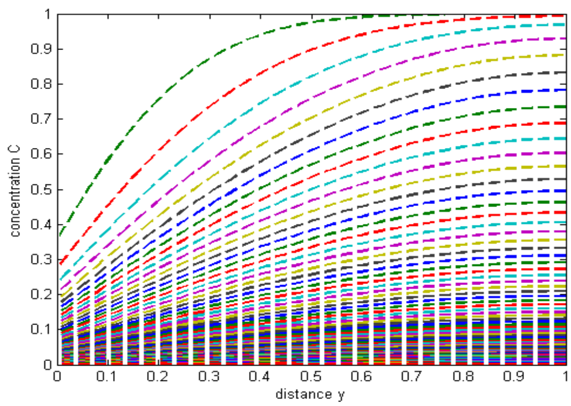

Fig. 7: Shows how concentration decreases as it get past the membrane.

Along the distance y of Fig. 7 conforms to our earlier assertion on accumulation of waste close to the base of the membrane. It is noteworthy that concentration tends towards zero at the base of the membrane due to diffusion but it's never zero. This is quickly shown by 'zooming in' Fig. 7 above.

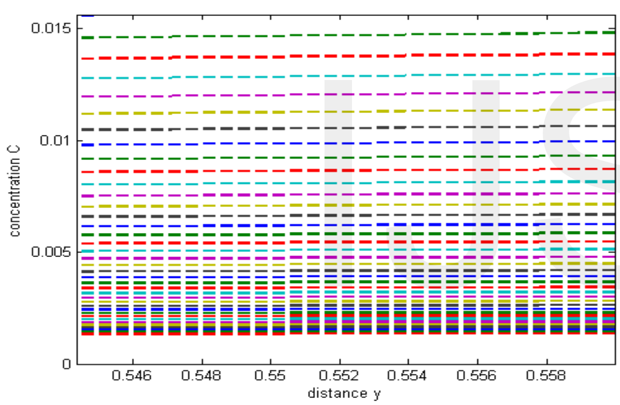

Fig. 8: A 'zoom in' in Fig. 7 to justifying 'non-zeroness' of concentration on the membrane over time during the haemodialysis.

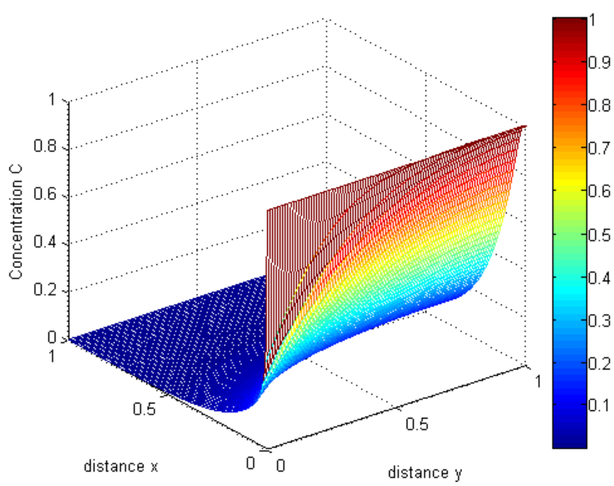

(b) Further illustration of numerical solution using MATLAB's mesh command. This magnifcently represents different range of values assumed by C as it moves down the concentration gradient.

Though we have demystified the main features of our model solution, the fact that we are yet to understand the efficiency of our model is of great concern. However, a critical look in Appendix C Tables 4 and 5 informs that the two most sensitive model parameters are α_b and β_b since slight changes in them would lead to a significant variance in the efficiency of our model.

These overwhelming changes shown in Tables 4 and 5 of Appendix C for selected values of the parameters unravel how deficient the estimated values of β_b and α_b in Table 2 could be since a decrease in these parameters could probably lead to decrease in efficiency and vice-versa. In particular, to achieve an efficiency of 100% with a fixed $\beta = 7$, a choice of $\alpha = 19.7$ is sufficient though with minute proportion of waste undiffused out while $\alpha = 392.1$ gives a total waste clearance with the same efficiency as the former.

Similarly, for a fixed $\alpha_b = 3.2$, $\beta_b = 20280$ gives a total waste clearance with 100% efficiency while $\beta_b = 55000$ gives the same efficiency but with minute traces of waste leaving with the blood. It is worthy of note from Table 5 that as $\beta_b \to \infty$, the concentration out of the haemodialyser behaves erratic resulting in regimes of minute traces of waste in blood and total waste clearance with efficiency maintained at 100%. This is expected since from [2] different waste molecules diffuse at different rates.

Hence, to achieve 100% efficiency with total waste clearance, one would expect that values of β_b ranges as in Table 2 while α_b is allowed to grow as large as sensibly possible.

Earlier, we observed from Figures 2 and 3 that the analytic solution and numerical solutions did not coincide, thus leading to an expected relative error. Their Relative Percentage Error (RPE) have been shown in Table 6 and 7 of Appendix C for variations in β_b and α_b . Observe that for a fixed $\beta_b = 7$, variations in α_b is inversely proportional to RPEs. In particular, as α_b grows larger and larger away from $\alpha_b = 3.2$, RPE found to decrease upto powers of 8×10^4 approx. In other words, as $\alpha_b \to \infty$, RPE converges to 8×10^4 approx. while for a fixed $\alpha_b = 3.2$, RPE 'fluctuates' as one cannot emphatically conclude whether an increase or decrease in values of β_b would lead to an increase or decrease in RPE which further supports our earlier assertion on the choices for α_b and β_b.

These large RPEs associated with the model solution could be

ISSN 2229-5518

attributed to the error in the eigenvalues λ_n as shown in Appendix A. Here we have used $n=101$ eigenvalues which is less accurate compared to best approximation obtained when $n=10^{310}$. One may also suggest that even though the numerical solution may have converged and looked stable; it might be of great interest to investigate our problem using other numerical scheme.

5. Conclusions

This research has investigated a mathematical model on haemodialysis which is the process by which excess waste in the blood are removed by physical passage of blood through a haemodialyser to remove waste by the processes of convection and diffusion. This alternative to waste removal is due to kidney dysfunction.

Haemodialysis is affected heavily by the concentration gradient, surface area of the membrane and distance travelled along the haemodialyser. For our purpose, we envisaged that the haemodialyser is a two-channeled device partitioned into two halves by a rectangular semi permeable membrane with blood and the dialysate flowing in a counter-clockwise direction on both sides of the channel.

We also saw that our objective was to develop a mathematical model capable of determining the efficiency of our device. This we have done using asymptotic and numerical approaches to obtaining the solution of the governing convection-diffusion equation coupled with suitable initial and boundary conditions.

Sensible assumptions were also imposed on the model for simplicity by assuming the flow field is unidirectionally constant in the x-direction; no influx from the dialysate region into the blood region; and the dialysate made to be zero on the membrane. Furthermore, we also used the fact that blood is an incompressible fluid and that no reasonable diffusion takes place along the z-direction. These assumptions simplified the concentrations in Ω_b and Ω_d to only functions of x, y and t.

Our governing equations were nondimensionalised by introducing scaling after which the six dimensional variables reduced to five dimensionless parameters. The values of the dimensionless parameter were calculated from values of the dimensional parameters. In particular, we used the fact that the speed on both sides of the channel is the ratio of mass flow rate to the area of the channel.

Asymptotic analysis was also considered in the limit of the smallest dimensionless parameter $\varepsilon \to 0$ which further reduced our governing equation and the prescribed boundary conditions on x. Thus informing us that there is no significant diffusion taking place along the x- direction.

The reduced problem from asymptotic analysis were solved for both steady and unsteady state solution analytically - separation of variables and Laplace transform accordingly; and numerically - MATLAB's $pdepe$. In particular, analytic solution to unsteady state was solved first by Laplace transform then followed by method of separation of variables with solution posed analogously to the solution of steady state. It was later transformed back to time space using Laplace inverse transform.

The unsteady state solution informed that concentration in the channel attains steady state in one time unit. Discontinuities associated with the membrane were also seen in the solution. A key note is that in the absence of the Heaviside function, the unsteady state solution assumes the steady state solution.

The eigenvalues were found to be in a transcendental equation and were preferably obtained using MATLAB's $fsolve$ with tolerance set to 10^{-6}. The solution obtained revealed that the eigenvalues $\lambda_n = n\pi + \text{correction}(\varepsilon)$. It was also justified asymptotically that $\lambda_n \sim n\pi$ and can be shown using MATLAB that λ_n's were only a good approximation of eigenvalues for $n=10^{310}$.

Various plots of the steady state solutions were shown ranging from $2D \to 3D$. They all gave useful insights on the behaviour of the blood concentration as it flows down the concentration gradient and along the axial direction. It was worthy of note that the blood concentration moves in layers having its maximum close to the base of the membrane thus suggesting that different molecules of blood travel at different convection and diffusion rates. Consequently, for optimal performance there is need for increased large surface area to effectively capture and allow for diffusion of regimes of interest. Additionally, this maximum concentration was attributed to the fact that the waste molecules were being pulled closer by the dialysate concentration on the other side of the channel.

We also anticipated that at certain time on the flow regime, the waste concentration out of the channel would probably be zero and observed that it took quite some time initially for the membrane to completely absorb the waste before attaining steady state.

It was also shown that at no time in the flow regime the concentration on the membrane was zero. This insight begs for the question:

(Q1) How much waste is allowed on the membrane over time?

This question motivated the quest to determining the efficiency of our model since for a fixed inlet concentration, knowledge of the outlet concentration at the end of the channel will help inform of the quantity of waste that have diffused out.

The efficiency of the device was investigated by varying the parameters α_b and β_b as we saw that the only sensible choice of values for β_b were those in Table 2 while α_b could be allowed to grow as large as sensibly possible in other to achieve 100% efficiency with total waste clearance.

One prominent observation made was the analytic and numerical solution did not coincide thus begs for the fundamental question:

(Q2) Why the large disparity between the analytic and numerical solution?

To have a feel of (Q2), we were prompted to calculate RPE between them. It was pertinent to note that for a fixed $\alpha_b = 3.2$, RPE 'fluctuates' as one could not emphatically conclude whether an increase or decrease in values of β_b would lead to an increase or decrease in RPE which further gave a formidable backbone to our assertion on the choices of α_b and β_b for optimal haemodialyser performance.

Q1 and Q2 remains an open question though we have made the following suggestions:

- Large RPEs associated with the model could be attributed to the error in eigenvalues.
- MATLAB's *pdepe* have converged and looked stable but further insight could be obtained by investigating the problem using other numerical scheme.
- A detailed modeling of the membrane since the norm from the analytic solution were seen to be very small compared to the numerical solutions.

Possible limitations of our model

- Less attention on the membrane and the dialysate. Dwelt mainly on what was happening in the blood domain.
- No attention was paid on other components of the haemodialysis set up as shown in Fig. 1. In particular how pressure controls could be used to control flow rates which in turn controls the velocity field.
- Did not consider different flow rates for different molecules of blood. It generally assumed that all waste molecules in blood have the same diffusion and convection rates.
- Suitable for a known fixed inlet concentration.

A brief review of [4], [5] showed that hollow (cylindrical) fiber membranes were commonly used. Particular attempts were made by [4] to model the velocities and pressure of blood and dialysate in the dialyser as well as the concentration of blood cells using a single hollow fiber and dialysate flowing outside it. They found out that varying the pressure in the dialysate moved the location at which the maximum blood concentration was archived, and that the maximum blood concentration was directly proportional to the product of the blood cell Peclet number and permeability of the membrane. It is worthy of note that the blood plasma and the dialysate were assumed to be Stokes flow while the pressure gradient varied only in the axial direction with concentration considered as a continuous scalar field.

Though our model correctly models the efficiency of our device, it however came with great price of high relative percentage error. It's worth extending our model to problems for pressure and velocities of blood and dialysate; and comparing with results in [4] to determine the suitability of a hollow cylindrical membrane and rectangular membrane with regards to efficiency.

Appendix A . Steady State

Consider the decoupled system (3.13), (3.14) and (3.16). Assume that blood flow is steady. Then the decoupled system becomes:

$$\frac{\partial C_0}{\partial x} = \alpha_b \frac{\partial^2 C_0}{\partial y^2} \tag{A.1}$$

ICs:

$$x = 0: \quad C_0 = 1 \tag{A.2}$$

BCs:

$$y = 0: \quad \frac{\partial C_0}{\partial y} = \beta_b C_0; \qquad y = 1: \quad \frac{\partial C_0}{\partial x} = 0 \tag{A.3}$$

To find the analytic solution of (A.1), we adopt method of separation of variables.

Define:

$$C_0(x, y) = X(x)Y(y) \tag{A.4}$$

Differentiating (A.4) w.r.t. x, y and substituting accordingly into (A.1) gives

$$\frac{1}{\alpha_b}\frac{X'}{X} = \frac{Y''}{Y} \tag{A.5}$$

Observe that both sides of (A.5) must be equal to a negative constant, say, $-\lambda^2$ in other for the solution to satisfy (A.1)-(A.3) without being identically zero. Hence

$$\frac{1}{\alpha_b}\frac{X'}{X} = \frac{Y''}{Y} = -\lambda^2 \tag{A.6}$$

i.e.

$$X' + \alpha_b \lambda^2 X = 0; \quad Y'' + \lambda^2 Y = 0 \tag{A.7}$$

On solving (A.7), we get

$$X(x) = A_1 e^{-\alpha_b \lambda^2 x}; Y(y) = A_2 cos\lambda y + B_2 sin(\lambda y);$$
$$C_0(x, y) = e^{-\alpha_b \lambda^2 x}\left(Acos(\lambda y) + Bsin(\lambda y)\right) \tag{A.8}$$

Applying (A.3a) to (A.8c) gives

$$-A\lambda sin(\lambda y) + B\lambda cos(\lambda y) = \beta_b\left(Acos(\lambda y) + Bsin(\lambda y)\right) \tag{A.9}$$

At $y = 0$, (A.9) gives

$$\frac{B}{A} = \frac{\beta_b}{k} \tag{A.10}$$

Also, on imposing (A.3b) on (A.8c):

$$-A\lambda sin(\lambda y) + B\lambda cos(\lambda y) \tag{A.11}$$

At $y = 1$, (A.11) simplifies to

$$tan(\lambda) = \frac{B}{A}; \quad i.e. \quad B = Atan(\lambda) \tag{A.12}$$

Substitute (A.10) into (A.12):

$$tan(\lambda) = \frac{\beta_b}{\lambda} \quad \text{(A.13)}$$

Observe from the foregoing that (A.8c) is just a solution to (A.1). Thus the fundamental solution to (A.1) is

$$C_0(x,y) = \sum_{n=0}^{\infty}\left(A_n cos(\lambda_n y) + B_n sin(\lambda_n y)\right)e^{-\alpha_b \alpha_n^2 x} \quad \text{(A.14)}$$

Impose (A.12) on (A.14):

$$C_0(x,y) = \sum_{n=0}^{\infty} A_n\left(cos(\lambda_n y) + tan(\lambda_n) sin(\lambda_n y)\right)e^{-\alpha_b \alpha_n^2 x} \quad \text{(A.15)}$$

Also from (A.2), at $x = 0$, (A.15) gives the relation

$$C_0(x,y) = \sum_{n=0}^{\infty} A_n\left(cos(\lambda_n y) + tan(\lambda_n) sin(\lambda_n y)\right) = 1 \quad \text{(A.16)}$$

Recall: $tan(\lambda_n) = \dfrac{sin(\lambda_n)}{cos(\lambda_n)}$ and

$cos\left(\lambda_n(1-y)\right) = cos(\lambda_n)cos(\lambda_n y) + sin(\lambda_n)sin(\lambda_n y)$.

Substituting them into (A.15)-(A.16) gives

$$\sum_{n=0}^{\infty}\left(\frac{cos\left(\lambda_n(1-y)\right)}{cos\lambda_n}\right) = 1;$$
$$C_0(x,y) = \sum_{n=0}^{\infty} A_n\left(\frac{cos\left(\lambda_n(1-y)\right)}{cos\lambda_n}\right)e^{-\alpha_b \lambda_n^2 x} \quad \text{(A.17)}$$

Orthogonality of Functions:

To find an expression for A_n we use the orthogonality of $\{cos(\lambda_n y),\ n = 0,1,2,...\}$ in the sense that

$$\int_0^1 cos(\lambda_n y)cos(\lambda_m y)dy = \begin{cases} \int_0^1 cos(\lambda_n y)cos(\lambda_m y)dy & m \neq n, m = n = 0 \\ \dfrac{1}{4\lambda_m}\left(2\lambda_m + sin(2\lambda_m)\right) & m = n \end{cases}.$$

since for $m = n$:

$$\int_0^1 cos(\lambda_n y)cos(\lambda_m y)dy = \int_0^1 cos^2(\lambda_m y)dy$$
$$= \frac{1}{2}\int_0^1\left(1 + cos(2\lambda_m y)\right)dy$$
$$= \frac{1}{2}\left[y + \frac{sin(2\lambda_m y)}{2\lambda_m}\right]_0^1 = \frac{1}{4\lambda_m}\left(2\lambda_m + sin(2\lambda_m)\right) \quad \text{(A.18)}$$

such that:

$$A_m = \frac{4\lambda_m cos(\lambda_m)}{2\lambda_m + sin(2\lambda_m)}\int_0^1 cos(\lambda_m y)dy$$
$$= \left[\frac{4\lambda_m cos(\lambda_m)}{2\lambda_m + sin(2\lambda_m)}\right]\frac{1}{\lambda_m}[sin(\lambda_m y)]_0^1$$
$$= \left[\frac{4\lambda_m cos(\lambda_m)}{2\lambda_m + sin(2\lambda_m)}\right]\frac{sin\lambda_m}{\lambda_m} = \left[\frac{2sin(2\lambda_m)}{2\lambda_m + sin(2\lambda_m)}\right] \quad \text{(A.19)}$$

The eigenvalues $\lambda_m \in (n\pi, (n+\frac{1}{2}))$, $n = 0,1,2,...,$ were obtained numerically using MATLAB's *fsolve* with initial guess $\lambda_0 = \pi/4 : pi : 401\pi/4$.

Next we justify that $\lambda_n = n\pi + correction(\varepsilon) \sim n\pi$ as $n \to \infty$. Substitute $\lambda_n = n\pi + \varepsilon$ into $tan\lambda_n = \dfrac{\beta_b}{\lambda_n}$ to obtain

$$tan(n\pi + \varepsilon) = \frac{\beta_b}{n\pi + \varepsilon} \quad \text{(A.20)}$$

Trigonometry identity: $tan(a+b) = \dfrac{tan(a) + tan(b)}{1 - tan(a)tan(b)}$.

Clearly, (A.20) becomes $tan(n\pi + \varepsilon) = \dfrac{tan(n\pi) + tan(\varepsilon)}{1 - tan(n\pi)tan(\varepsilon)}$.

Since $tan(n\pi)$ is small relative to $tan(\varepsilon)$, (A.20) reduces to

$$tan(\varepsilon) \approx \frac{\beta_b}{n\pi + \varepsilon} \quad \text{(A.21)}$$

Pose: $\varepsilon \sim \varepsilon_0 + \varepsilon_1 + \varepsilon_2 + ...$

Use the fact that $tan(\varepsilon) \approx \varepsilon$ and $(1+y)^{-1} \approx 1 - y + y^2 - ...$ to obtain that

$$\varepsilon_0 + \varepsilon_1 + \varepsilon_2 + ... \approx \frac{\beta_b}{n\pi}\left(1 - \frac{\varepsilon}{n\pi} + \frac{\varepsilon^2}{(n\pi)^2} - \frac{\varepsilon^3}{(n\pi)^3} + ...\right).$$

i.e.

$$\varepsilon_0 \approx \frac{\beta_b}{n\pi}, \varepsilon_1 \approx \frac{\beta_b}{(n\pi)^2}, \varepsilon_2 \approx \frac{\beta_b}{(n\pi)^3}, ... \quad \text{(A.22)}$$

As $n \to \infty$, $\varepsilon \to 0$. In other words, as n keeps increasing the value of ε becomes relatively small justifying our claim.

Appendix B Unsteady State

Again, consider the decoupled system (3.13), (3.14) and (3.16). To illustrate the transient behaviour of the decoupled system, we define the Laplace transform of $C_0(x,y,t)$ as

$$\bar{c}(x,y;s) = \int_0^{\infty} e^{-st}C_0(x,y,t)dt \quad \text{(B.1)}$$

Taking Laplace transform of the decoupled system gives

ISSN 2229-5518

$$sL\{C_0\}-C_0(x,y,0)+L\{\frac{\partial C_0}{\partial x}\}=\alpha_b L\{\frac{\partial^2 C_0}{\partial y^2}\} \quad \text{(B.2)}$$

IC: $x=0:\ \bar{c}=\frac{1}{s}$;

BCs: $y=0:\ \frac{\partial \bar{c}}{\partial y}=\beta_b \bar{c},\ \ y=1:\ \frac{\partial \bar{c}}{\partial y}=0$.

Apply (3.14a) to (B.2) to get

$sL\{C_0\}+L\{\frac{\partial C_0}{\partial x}\}=\alpha_b L\{\frac{\partial^2 C_0}{\partial y^2}\}$. By (B.1), we have

$$s\bar{c}+L\{\frac{\partial C_0}{\partial x}\}=\alpha_b L\{\frac{\partial^2 C_0}{\partial y^2}\} \quad \text{(B.3)}$$

From definition of Laplace transform (B.3) becomes

$$s\bar{c}+\int_0^\infty e^{-st}\frac{\partial C_0}{\partial x}dt=\alpha_b\int_0^\infty e^{-st}\frac{\partial^2 C_0}{\partial y^2}dt \quad \text{(B.4)}$$

Assume we can interchange integration and differentiation so that (B.4) is written as

$$s\bar{c}+\frac{\partial}{\partial x}\int_0^\infty e^{-st}C_0(x,y,t)dt=\alpha_b\frac{\partial^2}{\partial y^2}\int_0^\infty e^{-st}C_0(x,y,t)dt \quad \text{(B.5)}$$

Using (B.1), (B.5) gives:

$$s\bar{c}+\frac{\partial \bar{c}}{\partial x}=\alpha_b\frac{\partial^2 \bar{c}}{\partial y^2} \quad \text{(B.6)}$$

Multipy both sides of (B.6) by e^{sx} to get

$$\frac{\partial(e^{sx}\bar{c})}{\partial x}=\alpha_b\frac{\partial^2(e^{sx}\bar{c})}{\partial y^2} \quad \text{(B.7)}$$

set $v(x,y)=e^{sx}\bar{c}(x,y;s)$. Then

$$\frac{\partial v}{\partial x}=\alpha_b\frac{\partial^2 v}{\partial y^2} \quad \text{(B.8)}$$

Next, we derive IC and BCs as follows:

IC:

$$x=0:\ \ v=e^{x.0}\frac{1}{s}=\frac{1}{s} \quad \text{(B.9)}$$

BCs:

$$y=0:\ \ \frac{\partial v}{\partial y}=e^{sx}\frac{\partial \bar{c}}{\partial y}=e^{sx}\beta_b e^{-sx}v=\beta_b v$$
$$y=1:\ \ \frac{\partial v}{\partial y}=e^{sx}\frac{\partial \bar{c}}{\partial y}=0 \quad \text{(B.10)}$$

Observe that the system (B.8)-(B.10) is analogous to steady state decoupled system. Thus, the general solution to (B.8) is given by $v(x,y)=\sum_{n=0}^{\infty}A_n\left(\frac{\cos(\lambda_n(1-y))}{\cos(\lambda_n)}\right)e^{-\alpha_b\lambda_n^2 x}$ so that

$$\bar{c}(x,y;s)=e^{-sx}\sum_{n=0}^{\infty}A_n(s)\left(\frac{\cos(\lambda_n(1-y))}{\cos\lambda_n}\right)e^{-\alpha_b\lambda_n^2 x} \quad \text{(B.11)}$$

Impose (B.9) on (B.11) to obtain

$\sum_{n=0}^{\infty}A_n(s)\left(\frac{\cos(\lambda_n(1-y))}{\cos(\lambda_n)}\right)=\frac{1}{s}$. Next we transform back to time space using Laplace inverse transform. i.e.

$$C_0(x,y,t)=L^{-1}\{\frac{1}{s}e^{-sx}\}\sum_{n=0}^{\infty}\hat{A}_n\left(\frac{\cos(\lambda_n(1-y))}{\cos\lambda_n}\right)e^{-\alpha_b\lambda_n^2 x}, \quad \text{(B.12)}$$

$$A_n(s)=\frac{1}{s}\hat{A}_n.$$

$$L^{-1}\{\frac{1}{s}\}\sum_{n=0}^{\infty}\hat{A}_n\left(\frac{\cos(\lambda_n(1-y))}{\cos(\lambda_n)}\right)=L^{-1}\{\frac{1}{s}\}=1$$
$$\Rightarrow\sum_{n=0}^{\infty}\hat{A}_n\left(\frac{\cos(\lambda_n(1-y))}{\cos(\lambda_n)}\right)=1 \quad \text{(B.13)}$$

(B.12) gives $u(t-x)\sum_{n=0}^{\infty}\hat{A}_n\left(\frac{\cos(\lambda_n(1-y))}{\cos(\lambda_n)}\right)e^{-\alpha_b\lambda_n^2 x}$ where $u(t-x)$ is a step function.

Appendix C Efficiency

Here we derive the equation for the efficiency of our model in terms of inlet and outlet blood concentrations. This is an important tool in analysing the quantity of waste removed by diffusion.

$$C_{in}=\iint_A C_0(x,y)\big|_{x=0}dA=\int_{y=0}^{1}\int_{z=0}^{1}C_0(x,y)\big|_{x=0}dydz$$
$$=\int_{y=0}^{1}\int_{z=0}^{1}1.dydz=1 \quad \text{(C.1)}$$

$$C_{out}=\iint_A C_0(x,y)\big|_{x=1}dA=\int_{y=0}^{1}\int_{z=0}^{1}C_0(x,y)\big|_{x=1}dydz$$
$$=\int_{y=0}^{1}\int_{z=0}^{1}\sum_{n=0}^{\infty}A_n\left(\frac{\cos(\lambda_n(1-y))}{\cos(\lambda_n)}\right)e^{-\alpha_b\lambda_n^2 x}\bigg|_{x=1}dydz$$
$$=\int_{y=0}^{1}\sum_{n=0}^{\infty}A_n\left(\frac{\cos(\lambda_n(1-y))}{\cos(\lambda_n)}\right)e^{-\alpha_b\lambda_n^2}dy$$
$$=\sum_{n=0}^{\infty}A_n e^{-\alpha_b\lambda_n^2}\int_{y=0}^{1}\left(\frac{\cos(\lambda_n(1-y))}{\cos(\lambda_n)}\right)dy$$
$$=\sum_{n=0}^{\infty}A_n e^{-\alpha_b\lambda_n^2}\left[\frac{\sin(\lambda_n(1-y))}{-\lambda_n\cos(\lambda_n)}\right]_0^1=$$

$$\sum_{n=0}^{\infty} A_n e^{-\alpha_b \lambda_n^2} \frac{tan(\lambda_n)}{\lambda_n} = \sum_{n=0}^{\infty} A_n e^{-\alpha_b \lambda_n^2} \frac{\beta_b}{\lambda_n^2}$$
$$= \sum_{n=0}^{\infty} \left[\frac{2sin(2\lambda_m)}{2\lambda_m + sin(2\lambda_m)} \right] e^{-\alpha_b \lambda_n^2} \frac{\beta_b}{\lambda_n^2} \quad \text{(C.2)}$$

$$\text{Efficiency} = \frac{C_{in} - C_{out}}{C_{in}} \times 100\% .$$

TABLE 4: Illustrates sensitivity of efficiency with respect to changes in α_b, $\beta_b = 7$ fixed and $C_{in} = 1$.

α_b	C_{out}	Efficiency $(C_{in} - C_{out})/C_{in} \times 100\%$
1	2.577538921207383e-006	99.999742246107886
3.2	3.986259600275664e-008	99.999996013740400
6.7	5.248105907026996e-011	99.999999994751903
10.5	3.913219454589593e-014	99.999999999996092
19.7	1.048983450321264e-021	100
100	8.559009727368343e-088	100
392.1	0	100
1000	0	100
30000	0	100
30001	0	100

TABLE 5: Illustrates sensitivity of efficiency with respect to changes in β_b, $\alpha_b = 3.2$ fixed and $C_{in} = 1$.

β_b	C_{out}	Efficiency $(C_{in} - C_{out})/C_{in} \times 100\%$
1	6.922968218290281e-007	99.999930770317818
4	8.993172345994621e-008	99.999991006827642
7	3.986259600275664e-008	99.999996013740400
15	1.818202341456285e-008	99.999998181797650
1000	7.596263185899565e-009	99.999999240373683
20280	0	100
20290	1.131673740535936e-282	100
55000	1.522354018193952e-036	100
55000	0	100

TABLE 6: Relative error in % between the analytic solution and numerical solution with varying α_b values, $\beta_b = 7$ fixed.

α_b	Analytical solution A	Numerical solution N	Rel. % Error $(N-A)/A \times 100\%$
1	0.042285806647024	48.778276448234152	1.152537801830430e+005
3.2	0.027332827872742	28.167414727863502	1.029534230084335e+005
6.7	0.020092505098798	20.145036908831308	1.001614497782872e+005
10.5	0.016886413411841	16.701228752004081	9.880335114200671e+004
19.7	0.014015229016223	13.317742915818149	9.492336993853016e+004
100	0.012169484353450	10.142222791805946	8.324143417449707e+004
392.1	0.012109110508274	10.049877023043969	8.289434558944000e+004
1000	0.012108945141049	10.049875621127658	8.289546743389353e+004
30000	0.012108945139410	10.049875621120890	8.289546744507557e+004
30001	0.012108945139410	10.049875621120890	8.289546744507557e+004

TABLE 7: Relative error in % between the analytic solution and numerical solution with varying β_b , $\alpha_b = 3.2$ fixed.

β_b	Analytical solution A	Numerical solution N	Rel. % Error $(N-A)/A \times 100\%$
1	0.033452895539359	46.192554560737371	1.379823806608612e+005
4	0.027355250436588	31.047372100046179	1.133969397264957e+005
7	0.027332827872742	28.167414727863502	1.029534230084335e+005
15	0.030131311563051	25.922513388928817	8.593181223852518e+004
1000	0.001158274260006	23.824395258810000	2.056787222779170e+006
20280	8.503314963183538e-006	23.792648174995303	2.798042854427288e+008
20290	6.904859568044099e-007	23.792647247878008	3.445782832065860e+009
55000	1.219961418152194e-007	23.791800849849345	1.950209274969474e+010
59000	1.643988303320489e-005	23.791764475390107	1.447196916635785e+008

Acknowledgment

Special thanks to Dr. Jonathan D. Evans of Department of Mathematical Sciences, University of Bath, UK for his commitments and inputs.

References

[1] *http://encyclopedia.thefreedictionary.com/Dialysis_cite_note-4*, Last accessed March 03, 2015.

[2] R.W. Harritton, *Principle of Dialysis: Diffusion, Convection and Dialysis Machine*, http://www.kidneyatlas.org /books5/adk5-01.ccc.QXD.pdf. Accessed May 02, 2015.

[3] A.Y. Christian and S. Hartmut, *Mathematical Biology II Lecture Notes MA30063*, University of Bath, Semester 2, 2015/2016.

[4] K. Haas, *Modeling Blood Cell Concentration in Dialysis Cartridge*, An MSc project submitted to Worcester Polytechnic Institute, 2010, https://www.wpi.edu/Pubs/ETD/Available/etd-42810-95415/unrestricted/MastersProject.pdf.

[5] H.E. Abaci, *Modelling Haemodialysis Operation*, An MSc project submitted to the Graduate School of Engineering and Sciences, İzmir Institute of Technology, 2008. http://library.iyte.edu.tr/tezler/master/kimyamuh/T000713.pdf.